Article

# Mechanistic Insights into Photodynamic Regulation of Adenosine 5′-Triphosphate-Binding Cassette Drug Transporters

Barry J. Liang, Sabrina Lusvarghi, Suresh V. Ambudkar,* and Huang-Chiao Huang*
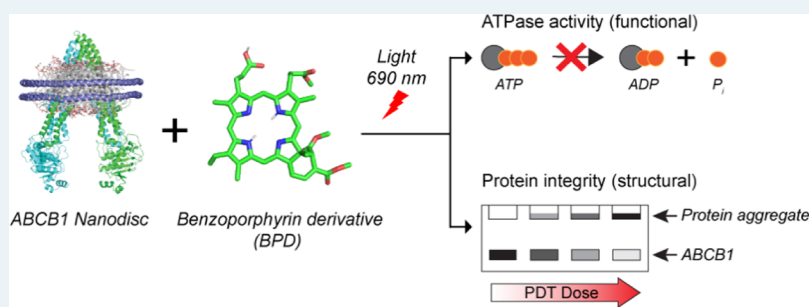
Read Online

ACCESS | Metrics & More | Article Recommendations | Supporting Information

**ABSTRACT:** Efforts to overcome cancer multidrug resistance through inhibition of the adenosine triphosphate-binding cassette (ABC) drug transporters ABCB1 and ABCG2 have largely failed in the clinic. The challenges faced during the development of non-toxic modulators suggest a need for a conceptual shift to new strategies for the inhibition of ABC drug transporters. Here, we reveal the fundamental mechanisms by which photodynamic therapy (PDT) can be exploited to manipulate the function and integrity of ABC drug transporters. PDT is a clinically relevant, photochemistry-based tool that involves the light activation of photosensitizers to generate reactive oxygen species. ATPase activity and *in silico* molecular docking analyses show that the photosensitizer benzoporphyrin derivative (BPD) binds to ABCB1 and ABCG2 with micromolar half-maximal inhibitory concentrations in the absence of light. Light activation of BPD generates singlet oxygen to further reduce the ATPase activity of ABCB1 and ABCG2 by up to 12-fold in an optical dose-dependent manner. Gel electrophoresis and Western blotting revealed that light-activated BPD induces the aggregation of these transporters by covalent cross-linking. We provide a proof of principle that PDT affects the function of ABCB1 and ABCG2 by modulating the ATPase activity and protein integrity of these transporters. Insights gained from this study concerning the photodynamic manipulation of ABC drug transporters could aid in the development and application of new optical tools to overcome the multidrug resistance that often develops after cancer chemotherapy.

**KEYWORDS:** *photodynamic therapy, cancer drug resistance, ABCB1, ABCG2, ATPase activity, protein cross-linking*

Adenosine triphosphate-binding cassette (ABC) transporters are a superfamily of membrane proteins found in almost all tissues and cells.[1] Many of these transporters serve as the first line of cellular defense against xenobiotics and metabolites. P-glycoprotein (P-gp/ABCB1) and breast cancer resistance protein (BCRP/ABCG2) are two prominent members of the ABC transporter superfamily expressed by a number of cancer types.[2] The overexpression of ABCB1 and ABCG2 in cancer cells has been associated with multidrug resistance and linked to poor chemotherapy outcomes in patients.[3] These ABC drug transporters utilize energy from adenosine 5′-triphosphate (ATP) binding and hydrolysis to efflux a wide range of chemically and structurally dissimilar cytotoxic drugs across cellular membranes against a concentration gradient. Despite being the subject of study for over 4 decades, none of the various methods of ABCB1 and ACBG2 inhibition investigated have proven to be successful in the clinic.[3]

The transport functions of both ABCB1 and ABCG2 rely on the coupling of ATP binding, protein conformation change, and ATP hydrolysis. The monomeric structure of ABCB1 and the dimer of ABCG2 consist of two transmembrane domains (TMDs) containing the substrate-binding pockets and two nucleotide-binding domains (NBDs), where ATP binding and hydrolysis occur.[4,5] When at rest, the transporter assumes an inward-facing conformation with the NBDs separated. ATP binding induces the dimerization of the NBDs, with the TMDs in an outward-facing conformation, which allows the substrate to be translocated from the cytosol to the extracellular matrix.
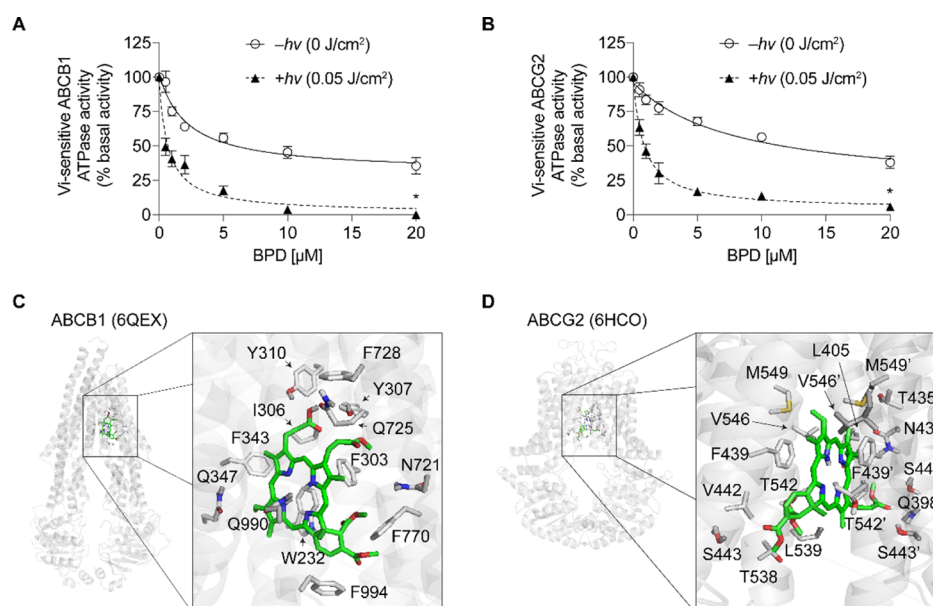
**Figure 1.** BPD inhibits the ATPase activity of ABCB1 and ABCG2 by binding to the substrate-binding pocket. The effect of BPD $(0-20\ \mu M)$ on vanadate $(V_i)$-sensitive ATPase activity of (A) ABCB1 and (B) ABCG2 was determined by the endpoint $P_i$ assay, as described in the Methods section. Data presented as mean $\pm$ standard deviation (SD) values from three independent experiments. ($n = 3$, $*P < 0.05$, two-tailed $t$-test. Asterisks denote significance compared to the no light groups). Molecular docking showing lowest energy binding poses of BPD docking to the cryo-electron microscopy structure of (C) human ABCB1 (PDB ID: 6QEX) and (D) human ABCG2 (PDB ID: 6HCO) via AutoDock Vina software. The photosensitizer BPD is presented in green for carbon, blue for nitrogen, red for oxygen, and gray for hydrogen. Interacting residues within 4 Å of the BPD are shown in gray sticks. Amino acids labeled with a prime symbol (′) indicate residues from the monomer two of ABCG2.

Subsequently, ATP hydrolysis occurs to reset the transporter to the inward-facing conformation. While it remains debatable if one or two ATPs are hydrolyzed per transport cycle, it is clear that both ATPase activity and protein structural integrity are crucial to the proper functioning of ABC drug transporters. Thus far, the development of inhibition strategies against ABCB1 and ABCG2 has focused on modulating the protein conformation and the ATPase activity with "always-on" small-molecule inhibitors.[6] These inhibitors, such as valspodar, tariquidar, and zosuquidar, have not succeeded in the clinic because of a lack of a therapeutic window for selective transporter blockage and due to non-specific toxic effects. The failure of inhibitors suggests that a conceptual shift is needed for a new strategy that could more selectively inhibit ABC drug transporters.

Light-activated chemical reactions have been demonstrated as one way to better control biological processes due to their unmatched spatial and temporal precision.[7] Photosensitization is a photochemical reaction mediated by a light-absorbing molecule that is not the ultimate target. An excellent example of a clinical application of photochemistry is photodynamic therapy (PDT), which involves the light activation of photosensitizers to generate reactive oxygen species to treat various diseases such as actinic keratosis, non-small cell lung cancer, and head and neck cancer.[8−10] In addition to treating primary diseases originating in a particular part of the body, PDT can be leveraged to target disseminated diseases with appropriate drug delivery carriers, targeting moieties, and optical technologies. For example, a study by Shimada et al. combined a phospholipid polymer with a photosensitizer to treat sentinel lymph node metastasis of breast cancer.[11] In another study, intralipid infusion was used to scatter light for activation of photosensitizers in the peritoneal cavity for the treatment of disseminated cancer.[12,13] Many photosensitizers

that have been successfully employed in the clinic, including chlorin e6, protoporphyrin IX, and benzoporphyrin derivative (BPD, aka. verteporfin), have been identified as substrates of ABCB1 and/or ABCG2.[14−18] This led us to formulate the hypothesis that the light activation of photosensitizers associated with ABC drug transporters might allow direct photochemical manipulation of the transporters' ATPase activity and protein integrity. The selective inhibition of ABC drug transporters by PDT is made possible by a combination of three important factors: a localized photosensitizer, spatiotemporal confinement of light, and the short half-life and travel distance of the reactive oxygen species.[19] Recently, we have shown that light activation of the photosensitizer BPD reduces the expression of ABCG2 transporters in pancreatic cancer cells and improves drug accumulation in cells and tumor tissues.[20] A study by Mao et al. also demonstrated that targeted PDT using photosensitizer-conjugated anti-ABCB1 antibody can selectively deplete chemo-resistant tumors.[21] While encouraging, the fundamental principles governing photochemical manipulation of ABC drug transporter activity and integrity remained unknown.

Here, we systematically evaluate how photochemistry directly impacts the function of ABC drug transporters at the molecular level. We use a combination of *in silico* molecular docking analysis, biochemical assays using High Five cell membrane vesicles, and lipid bilayer nanodiscs reconstituted with purified transporters to investigate the mechanism through which PDT inhibits the transporters' function. We demonstrate that optical activation of BPD reduces the ATPase activity of ABCB1 and ABCG2 in a light dose-dependent manner. Gel electrophoresis and western blotting show that light-activated BPD induces ABC drug transporter aggregation in part through covalent linkage. These results were not only confirmed using an FDA-approved BPD

photosensitizer but also with a next-generation lipidated formulation of BPD, (16:0) LysoPC-BPD. Insights into photochemical manipulation of ABC drug transporters will aid in the development and application of new optical tools to overcome the multidrug-resistant cancer that often develops after initial chemotherapy.

## ■ RESULTS

**Light Activation of Photosensitizers Attenuates the ATPase Activity of ABCB1 and ABCG2.** We have previously demonstrated that BPD photosensitizers can be readily transported by both ABCB1 and ABCG2 in drug-resistant human cancer cells.[18] Given that ABCB1- and ABCG2-mediated substrate transport is linked to ATP hydrolysis,[2,22] we investigated the effect of BPD on the vanadate (Vi)-sensitive ATPase activity of ABCB1 and ABCG2 in the absence and presence of light. We found that BPD alone, in the absence of light ($-h\nu$), modestly inhibited the ATPase activity of both transporters with half-maximal inhibition concentration ($IC_{50}$) values of $2.2 \pm 0.5$ and $7.9 \pm 2.1$ $\mu$M, respectively (Figure 1A,B, solid lines; Table S1). Light (690 nm, 0.05 J/cm$^2$, 50 mW/cm$^2$) activation ($+h\nu$) of BPD further reduced the ATPase activity of ABCB1 and ABCG2 by up to 12-fold, with $IC_{50}$ values of $0.7 \pm 0.1$ and $0.8 \pm 0.1$ $\mu$M, respectively (Figure 1A,B, dotted lines; Table S1). The decrease in ATPase activity of the transporters correlates with the increased production of reactive oxygen species (e.g., singlet oxygen) upon light activation of BPD (Figure S1). A thermal camera and thermocouple measurements confirmed that there is no increase in the sample temperature during light activation of BPD (Figure S2). These findings suggest that BPD alone and the production of reactive oxygen species upon its light activation inhibit the ATPase activity of ABCB1 and ABCG2.

**In Silico Analyses Support the Interaction of BPD with the Substrate-Binding Pockets of ABCB1 and ABCG2.** To further understand the site of the interaction between BPD and residues within the substrate-binding pockets of ABCB1 and ABCG2, we performed molecular docking analysis of BPD with the inward-facing conformation of human ABCB1 (PDB ID: 6QEX) and ABCG2 (PDB ID: 6HCO). The in silico docking analysis generated nine potential binding poses for BPD and the residues located within the substrate-binding pocket of ABCB1 (Figure S3) and ABCG2 (Figure S4). In all nine binding poses, the ABCB1 residues predicted to interact with BPD are aromatic and polar (Figure S3). Additionally, they are in transmembrane helices 5, 6, 7, and 12. These residues appear in at least 7 poses. In the case of ABCG2, BPD interacts with the hydrophobic and polar residues in transmembrane helices 2 and 5 (Figure S4). Figure 1C,D shows the lowest energy docking poses of BPD with substrate-binding pockets of ABCB1 and ABCG2. These molecular modeling data, in conjunction with the ATPase results, suggest that BPD interacts directly with the substrate-binding pockets of ABCB1 and ABCG2, modulating their ATPase activity.

**Light-Activated BPD Induces Aggregation of ABCB1 and ABCG2 Proteins.** To understand the mechanism of the effect of light activation of BPD on the function of these transporters, the impact of light-activated BPD on the level of monomeric ABCB1 and ABCG2 was evaluated using denaturing gel electrophoresis and immunoblotting. Figure 2 shows that light alone (690 nm, 5 J/cm$^2$, 50 mW/cm$^2$) or BPD
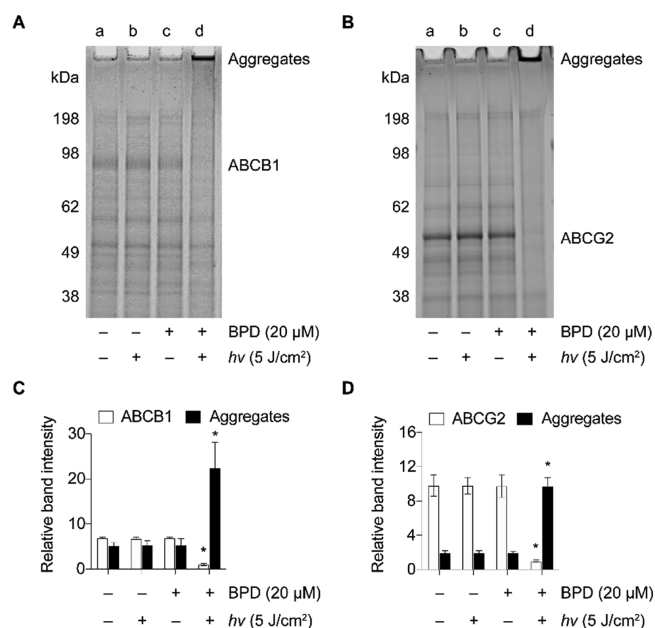


**Figure 2.** Light activation of BPD induces the aggregation of ABCB1 and ABCG2. Representative gels of (A) ABCB1 and (B) ABCG2 are shown with (a) no treatment, (b) 690 nm light ($h\nu$) only at 5 J/cm$^2$, (c) BPD only at 20 $\mu$M, and (d) BPD + 690 nm light. (C,D) Quantification of relative amounts of ABC drug transporter proteins and protein aggregates was done using ImageJ. Due to their hydrophobic nature, the ABCB1 and ABCG2 protein bands travel to lower molecular weight positions and do not appear at their true molecular weight positions. Data presented as mean $\pm$ SD values from three independent experiments. ($n = 3$, *$P < 0.05$, one-way analysis of variance (ANOVA), Tukey's post hoc test. Asterisks denote significance compared to the no treatment group).

alone (20 $\mu$M) did not alter the intensity of protein bands corresponding to monomeric (non-aggregated) ABCB1 and ABCG2. When the samples were treated with both light and BPD, the bands corresponding to monomeric ABCB1 and ABCG2 disappeared, and the aggregation of ABCB1 and ABCG2 became evident.

To further determine the thresholds for protein aggregation, we assessed monomeric ABCB1 and ABCG2, as well as protein aggregation, at various BPD concentrations (0−20 $\mu$M) and light fluences (690 nm, 0−5 J/cm$^2$, 50 mW/cm$^2$). Changes in the protein levels corresponding to the transporters were identified using colloidal blue staining of the proteins in the gels (Figure 3) and verified using immunoblotting with transporter-specific monoclonal antibodies (Figure S5). At a fixed optical fluence of 0.5 J/cm$^2$, BPD reduces the intensity of monomeric protein bands of ABCB1 and ABCG2 in a dose-dependent manner with $IC_{50}$ values of $1.8 \pm 0.2$ and $1.2 \pm 0.3$ $\mu$M, respectively (Figure 3A−D). Light alone (0.5 J/cm$^2$) did not alter the intensity of protein bands, and the intensity of protein bands corresponding to the aggregation of ABCB1 and ABCG2 only became evident when the BPD concentration was higher than 0.5 $\mu$M. Photochemical damage to ABC transporters was also observed in a light dose-dependent manner, as shown in Figure 3E−H. At a fixed BPD concentration of 2 $\mu$M, increasing light fluence from 0 to 5 J/cm$^2$ reduced the monomeric ABCB1 and ABCG2 band intensities by 9.1-fold and 5.4-fold, respectively. Correspondingly, this led to increased aggregation of these proteins.
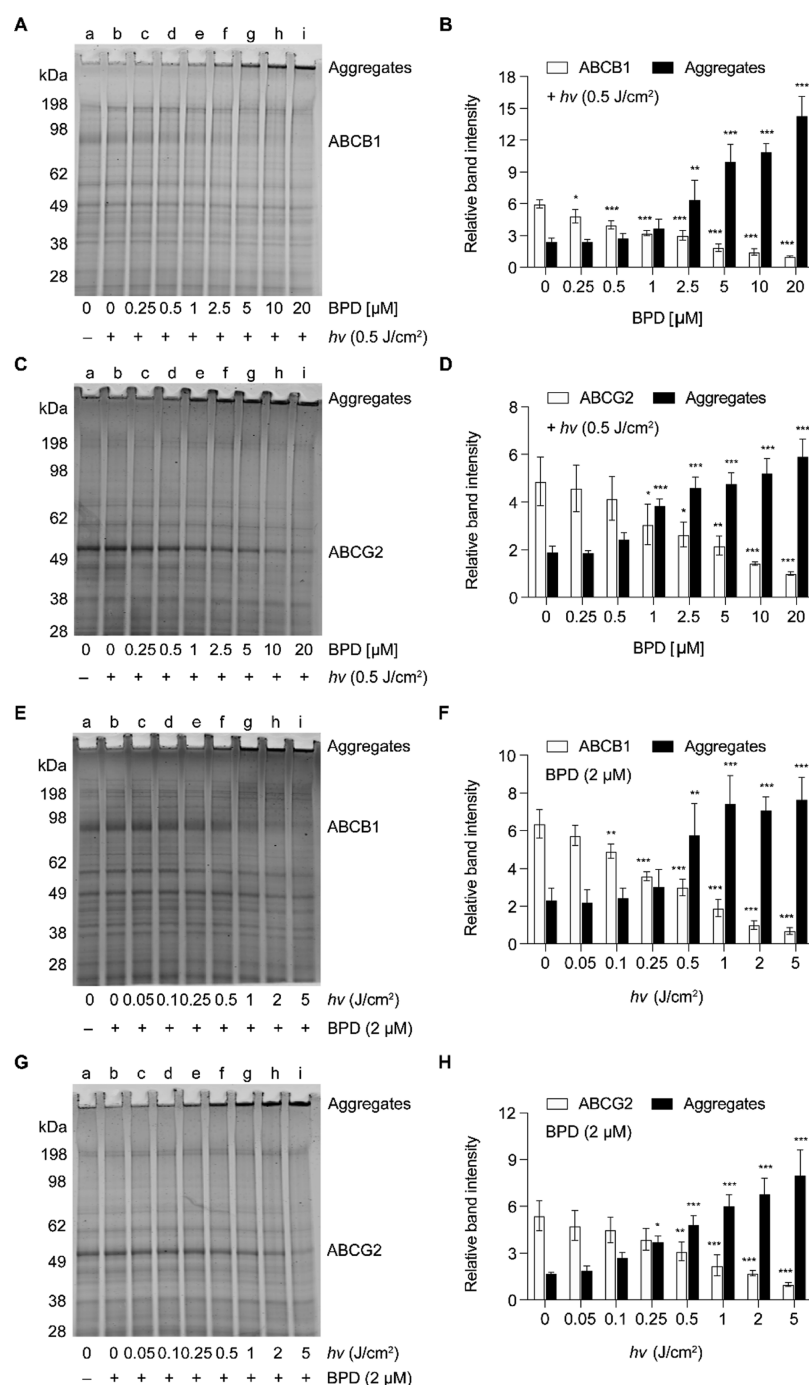
**Figure 3.** Photochemical damage to the ABCB1 and ABCG2 proteins in a BPD- and light dose-dependent manner. Membrane vesicles overexpressing ABCB1 or ABCG2 were exposed to BPD (0−20 μM) and light ($h\nu$; 690 nm, 0−5 J/cm$^2$, 50 mW/cm$^2$) prior to gel electrophoresis as described in the Methods section. (A−D) At a fixed fluence of 0.5 J/cm$^2$ and different BPD concentrations (0−20 μM), representative gels of (A) ABCB1 and (C) ABCG2 membrane vesicles: (a) no treatment; (b) 0; (c) 0.25; (d) 0.5; (e) 1; (f) 2.5; (g) 5; (h) 10; and (i) 20 μM of BPD. (B,D) Relative amounts of the ABC drug transporter proteins and protein aggregates were quantified using ImageJ. ($n = 3$, *$P < 0.05$, **$P < 0.01$, ***$P < 0.001$, one-way ANOVA, Tukey's post hoc test. Asterisks denote significance compared to the no BPD group). (E−H) At a fixed BPD concentration of 2 μM and different light fluences (690 nm, 0−5 J/cm$^2$), representative gels of (E) ABCB1 and (G) ABCG2 membrane vesicles: (a) no treatment; (b) 0; (c) 0.05; (d) 0.1; (e) 0.25; (f) 0.5; (g) 1; (h) 2; and (i) 5 J/cm$^2$ of light. (F,H) Quantification of relative amounts of ABC drug transporter proteins and protein aggregates was done using ImageJ. Data presented as mean ± SD values from three independent experiments. ($n = 3$, *$P < 0.05$, **$P < 0.01$, ***$P < 0.001$, one-way ANOVA, Tukey's post hoc test. Asterisks denote significance compared to the no light group).

## Assessment of Cysteine Cross-linking in Photochemistry-Induced Aggregation of ABCB1 and ABCG2.

Next, we studied the mechanism underlying the ABC drug transporter aggregation using 100 mM dithiothreitol (DTT) and 5 M urea (a protein unfolding agent). Membrane vesicles containing ABCB1 were subjected to photochemical sensitization (690 nm, 5 J/cm$^2$, 2 μM BPD) or heat treatment (100 °C for 3 min) to induce protein aggregation. Figure 4 shows that
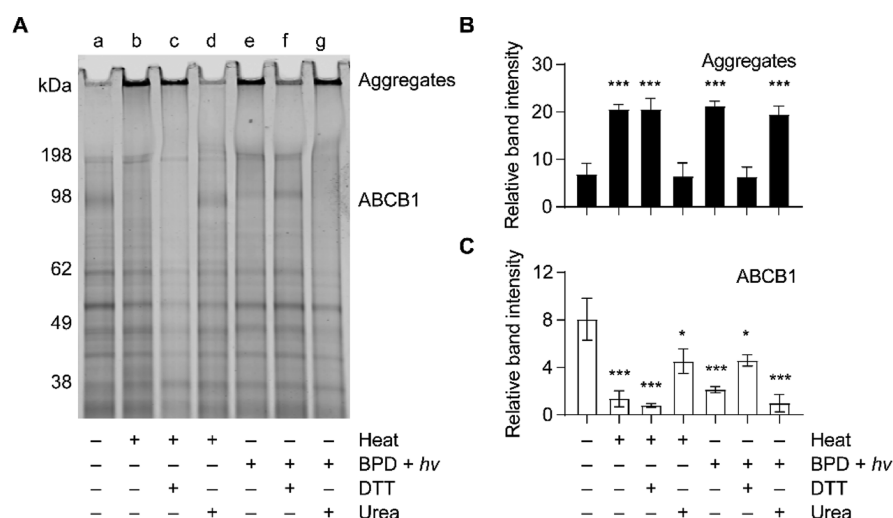
**Figure 4.** Light ($h\nu$) activation of BPD induces cross-linking in ABCB1 membrane vesicles. Membrane vesicles overexpressing ABCB1 were incubated with 2 $\mu$M BPD and light irradiated at 690 nm (50 mW/cm$^2$, 5 J/cm$^2$) prior to gel electrophoresis. Controls and addition of DTT (100 mM) or urea (5 M) were carried out as described in the Methods section. (A) Representative stained gel showing DTT reduces photochemistry-induced ABC transporter aggregation: (a) no treatment; (b) heat-treated; (c) heat-treated + DTT; (d) heat-treated + urea; (e) BPD + $h\nu$; (f) BPD + $h\nu$ + DTT; and (g) BPD + $h\nu$ + urea. Quantification of relative amounts of (B) protein aggregates and (C) ABCB1 was done using ImageJ. Data presented as mean ± SD values from three independent experiments. ($n$ = 3, *$P$ < 0.05, ***$P$ < 0.001, one-way ANOVA, Tukey's post hoc test. Asterisks denote significance compared to the no treatment group).

the addition of DTT reduced the photochemistry-induced ABCB1 aggregation, as the protein band corresponding to monomeric ABCB1 became evident. We suspected that disulfide bond formation was involved in the photochemistry-induced protein aggregation in ABCB1 membrane vesicles. However, further evaluation using a functional cysteine-less (cysless) ABCB1 mutant[23] showed a similar degree of protein aggregation, as well as a reduced intensity of the monomeric ABCB1 protein band, compared to that of wild-type ABCB1 (Figure S6). This indicates that the cysteine residues of ABCB1 are not involved in PDT-induced intramolecular cross-linking. In contrast, the addition of urea only reversed heat-induced protein aggregation but had no effect on photochemistry-induced protein aggregation. Due to a lack of intramolecular disulfide bond formation, it is possible that other intramolecular chemical bonds are responsible for the aggregation of ABCB1. The data in Figure S7 further show that the degree of photochemical inhibition of ATPase activity in cysless ABCB1 membrane vesicles is similar to that of wild-type ABCB1 membrane vesicles. This suggests that the binding of BPD to the cysless mutant is similar to that of wild-type ABCB1.

In contrast to ABCB1, the addition of DTT did not alter photochemistry-induced ABCG2 protein aggregation under the same conditions (Figure S8). We suspect that this is due to the difference in the number of cysteine residues in ABCG2 (24 cysteine residues in a functional dimer) and ABCB1 (7 cysteine residues). Thus, it is plausible that some of the cysteine residues are not accessible for DTT reduction. To confirm that a longer DTT incubation time does not reduce disulfide linkage, photochemically treated ABCG2 samples were incubated with the DTT for 24 h. Despite the longer DTT incubation period, the photochemistry-induced protein aggregation was not reduced (Figure S9). Similar to what was observed concerning ABCB1, while the addition of urea reversed heat-induced protein aggregation, it did not affect the photochemistry-induced protein aggregation. These results

suggest that the light activation of BPD also leads to protein covalent cross-linking of ABCG2 in membrane vesicles, and disulfide bond formation contributes minimally to ABCG2 protein aggregation.

**Photochemical Regulation of Purified ABCB1 Reconstituted in Nanodiscs.** Unlike membrane vesicles that contain other membrane proteins in addition to the ABC drug transporter of interest, the nanodisc model is engineered to only contain ABCB1 protein surrounded by lipids and stabilized by two small MSP1D1 belt proteins (Figure 5A).[24] The use of nanodisc models allows us to rule out the involvement of other membrane proteins in photochemical modulation of purified ABCB1. Like the membrane vesicle results, we observed that light activation of BPD attenuated the ATPase activity of ABCB1 in nanodiscs (Figure 5B). The ATPase activity of ABCB1 in nanodiscs was reduced by 51.7 ± 5.3 and 97.3 ± 1.3% in the absence and presence of light activation (690 nm, 0.05 J/cm$^2$, 50 mW/cm$^2$), respectively. Consistent with the membrane studies, we also found that light activation (690 nm, 50 mW/cm$^2$) of 2 $\mu$M BPD at 0.5 and 5 J/cm$^2$ induced protein aggregation and resulted in the disappearance of the protein band corresponding to monomeric ABCB1 by 49.0 ± 2.6 and 88.0 ± 3.5%, respectively (Figure 5C,D). Taken together, these data demonstrate that photosensitized BPD could directly affect the ATPase activity and the structural integrity of ABCB1 without the participation of any other membrane proteins.

Light activation of the lipidated photosensitizer is less effective as a modulator of ABCB1 and ABCG2. We observed that the lipidated BPD (16:0) LysoPC-BPD,[18] a weaker substrate of the ABC drug transporters, also interacts with residues within the substrate-binding pockets of ABCB1 (Figures 6A and S10) and ABCG2 (Figures 6B and S11). We tested the effect of (16:0) LysoPC-BPD on ATPase activity and the aggregation of ABCB1 and ABCG2. In the presence of (16:0) LysoPC-BPD (0−20 $\mu$M), the ATPase activity of ABCB1 displayed a biphasic dose response, with low
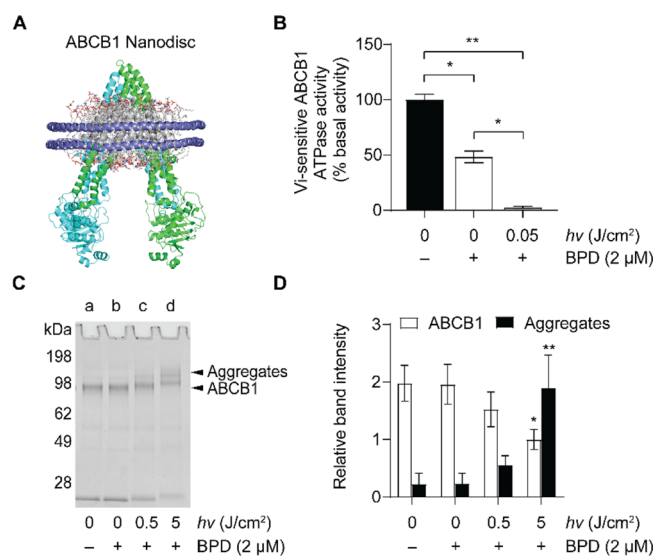
**Figure 5.** Light activation of BPD inhibits ATPase activity and induces protein aggregation in a purified ABCB1 nanodisc model. (A) Purified ABCB1 was reconstituted in lipid nanodiscs (grey) along with the belt protein MSP1D1 (purple). (B) ATPase activity of ABCB1 after treatment with BPD alone or BPD plus light was determined by the endpoint $P_i$ assay, as described in the Methods section. Data presented as mean ± SD values from three independent experiments. ($n = 3$, *$P < 0.05$, **$P < 0.01$, one-way ANOVA, Tukey's post hoc test). (C) Representative stained gel shows protein aggregation and ABCB1 disappearance with increasing fluence (0−5 J/cm$^2$); (a) no treatment; (b) BPD only; (c) BPD + 0.5 J/cm$^2$; and (d) BPD + 5 J/cm$^2$. (D) Relative amounts of ABCB1 and protein aggregates were quantified using ImageJ. Data presented as mean ± SD values from three independent experiments. ($n = 3$, *$P < 0.05$, **$P < 0.01$, one-way ANOVA, Tukey's post hoc test. Asterisks denote significance compared to the no treatment group).

doses being stimulatory (<0.5 $\mu$M) and high doses inhibitory (>0.5 $\mu$M) (Figure 6C). On the other hand, (16:0) LysoPC-BPD only inhibited the ATPase activity of ABCG2 up to 76% in a concentration-dependent manner with an IC$_{50}$ value of 8.0 ± 1.5 $\mu$M (Figure 6D; Table S1). Gel electrophoresis studies also showed that light activation of (16:0) LysoPC-BPD induced aggregation of ABCB1 and ABCG2 (Figure S12) in a concentration- and light dose-dependent manner. These studies suggest light activation of (16:0) LysoPC-BPD impairs the function and damages the structural integrity of ABCB1 and ABCG2, despite being a weakly transported photosensitizing agent compared to free form BPD.

## ■ DISCUSSION

Decades of research to decipher ABC transporter−drug interactions have improved our understanding of multidrug resistance and the design of effective inhibitors. Despite three generations of small-molecule inhibitors developed over 30 years of work, many were found to be marginally effective or excessively toxic when combined with chemotherapy, and thus have had limited success in treating cancer patients.[3] PDT offers a way to selectively mediate inactivation of ABC drug transporters without damaging normal tissues.[20,21,25]

While it is well-documented that PDT can reverse chemoresistance and synergize with chemotherapy,[26,27] its direct inhibitory effect on ABC drug transporter-mediated multidrug resistance was not known. This study reveals the fundamental principles governing the photochemical manipu-

lation of the function and structural integrity of ABCB1 and ABCG2 using the BPD photosensitizer and its lipidated derivative [i.e., (16:0) LysoPC-BPD]. BPD was selected not only because it is currently being tested in cancer patients but also because it is a substrate of ABCB1 and ABCG2. Our *in silico* docking analyses show that BPD interacts with residues in the drug-substrate binding pocket of ABCB1 in a manner similar to vincristine (another ABCB1 substrate), as reported in a recently published ABCB1 cryo-EM structure.[28] We have previously shown that (16:0) LysoPC-BPD is a weaker substrate of ABCB1 that is not subject to ABCG2-mediated efflux in cancer cells.[18] Here, our *in silico* results suggest that, like BPD, (16:0) LysoPC-BPD also binds to the substrate-binding pocket within the transmembrane region of ABCB1 and ABCG2. Compared to BPD, more residues from both monomers of ABCG2 interact with (16:0) LysoPC-BPD due to the addition of the phospholipid tail, thus leading to more molecular interactions. This could partly explain why (16:0) LysoPC-BPD avoids ABCG2 efflux.[18]

ATP hydrolysis plays a key role in the substrate translocation mechanism of ABCB1 and ABCG2. Many small-molecule modulators of ABCB1 (e.g., tariquidar, elacridar, and zosuquidar) have been shown to inhibit both drug transport and ATPase activity at sub-micromolar concentrations.[6] In this study, we found that BPD inhibits the ATPase activity of ABCB1 and ABCG2 at low micromolar concentrations, while (16:0) LysoPC-BPD exerts a biphasic effect on the ATPase activity of ABCB1. The stimulation of ABCB1 ATPase activity by concentrations below 0.5 $\mu$M of (16:0) LysoPC-BPD suggests that (16:0) LysoPC-BPD is a weak substrate of ABCB1. This agrees with the published reports that the modification of the hydrogen bonding acceptor on photo-sensitizers with macromolecules [e.g., (16:0) LysoPC] could mitigate ABC drug transporter-mediated efflux.[18,29] At concentrations above 0.5 $\mu$M, (16:0) LysoPC-BPD suppresses the ATPase activity of ABCB1. In the presence of light, both BPD and (16:0) LysoPC-BPD can generate reactive oxygen species to further reduce the ATPase activity of ABCB1 and ABCG2 by 2- to 12-fold. The use of light and photosensitizer to photochemically inhibit ATPase activity provides an additional layer of spatiotemporal control of ABC drug transporter activity.

Singlet oxygen plays an important role in direct photo-chemical oxidation and cross-linking of proteins, particularly at the cysteine, histidine, tryptophan, and tyrosine residues.[30−33] For instance, it has been demonstrated that singlet oxygen molecules react with cysteines to produce peroxide-like RS$^+$−OO$^-$ species.[34] Subsequently, these RS$^+$−OO$^-$ species undergo adduct formation and result in disulfide bonds.

Disulfide bond formation may play a role in the aggregation of ABCB1, as C431 and C1074 in the Walker A sequence can form an intramolecular disulfide bond that leads to ABCB1 aggregation.[35] However, we found no significant difference in ABCB1 aggregation between wildtype and cysless ABCB1 after PDT. This suggests disulfide linkage within ABCB1 or between ABCB1 and membrane proteins contributes minimally towards the aggregation of ABCB1. As addition of DTT minimized the degree of ABCB1 aggregation, this suggests that PDT reduces the number of disulfide bonds between membrane proteins. As shown with purified ABCB1 reconstituted into nanodiscs, PDT can induce direct structural damage to the transporter in the absence of other membrane proteins. The discrepancy between the degree of aggregation in the vesicle and nanodisc models
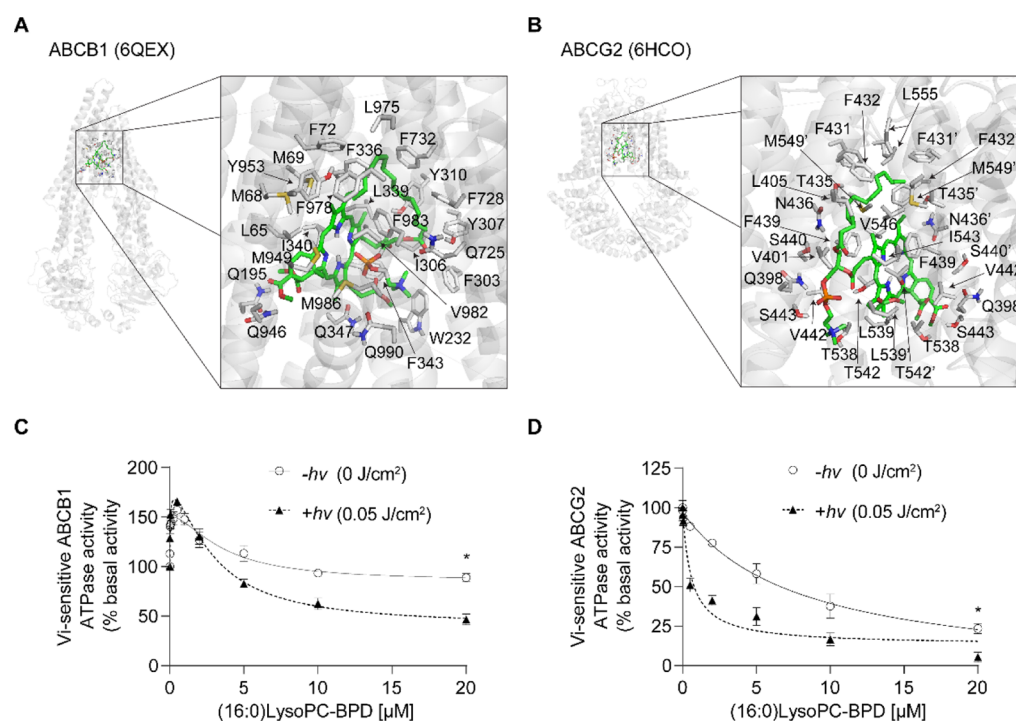
**Figure 6.** (16:0) LysoPC-BPD binds to the substrate-binding pockets of ABCB1 and ABCG2 and modulates the ATPase activity. (16:0)LysoPC-BPD was docked to the cryo-electron microscopy structure of (A) human ABCB1 (PDB ID: 6QEX) and (B) human ABCG2 (PDB ID: 6HCO) using AutoDock Vina software as described in the Methods section. (16:0) LysoPC-BPD is presented in green for carbon, blue for nitrogen, red for oxygen, and gray for hydrogen. Interacting residues within 4 Å of the BPD are shown in gray sticks. The effect of (16:0) LysoPC-BPD (0–20 $\mu$M) on vanadate ($V_i$)-sensitive ATPase activity of (C) ABCB1 and (D) ABCG2 was determined by the endpoint $P_i$ assay, as described in the Methods section. Light activation of (16:0) LysoPC-BPD (690 nm, 50 mW/cm$^2$, 0.05 J/cm$^2$) inhibits ATPase activity of ABCB1 and ABCG2. Data presented as mean ± SD values from three independent experiments. ($n = 3$, *$P < 0.05$, two-tailed $t$-test). Amino acids labeled with a prime symbol (′) indicate residues from the monomer two of ABCG2.

may be attributed to the difference in lipid content in the models. It is well-established that lipid peroxidation could occur in photodynamically damaged cells,[36,37] especially with hydrophobic photosensitizers, such as BPD and (16:0) LysoPC-BPD. This suggests that ABCB1 also might crosslink with other oxidized lipids and membrane proteins in the lipid bilayer after photosensitization. In contrast, DTT did not mitigate photochemistry-induced ABCG2 aggregation despite a longer incubation period. Although other cysteine-based crosslinks cannot be excluded, based on our results, it is reasonable to assume that disulfide bond formation contributes minimally to photochemistry-induced ABCG2 aggregation. Further studies are needed to investigate the histidine-, tryptophan-, and tyrosine-based crosslinks in photochemically modulated ABC drug transporters. Based on our findings, PDT-mediated protein cross-linking of ABCB1 and ABCG2 and inhibition of ATPase activity is the molecular basis for the inhibition of the efflux function of the ABCB1 and ABCG2 transporters. It is also important to note that photochemical modulation of ABC drug transporters occurs at low light irradiance levels in the mW/cm$^2$ range and does not depend on thermally induced "heating" of samples, thus eliminating the possibility of heat-induced protein aggregation.

Our analyses demonstrate that photochemical inhibition of ABCB1 and ABCG2 can be achieved through two mechanisms. A reduction of ATPase activity generally occurs at <1 $\mu$M × J/cm$^2$, followed by protein structural damage at higher doses (Table S2). Therefore, in principle, photochemical inhibition of ABC transporters can be precisely controlled to either affect the enzymatic activity or structural integrity of the protein. While this study focuses on understanding how photochemistry affects ABC drug transporters using membrane models that are free of cell organelles, photochemical modulation of mitochondria, the endoplasmic reticulum, and transcription factors (e.g., YAP/TAZ) could also lead to changes in the function or expression of ABC drug transporters in cells. Currently, there are few strategies to indirectly target ABC drug transporters via modulation of cellular organelles. We previously demonstrated that BPD-based PDT can induce mitochondrial depolarization[38] and disrupt the YAP/TAZ pathway.[39] This makes BPD an attractive candidate for both direct and indirect photochemical inhibition of ABCB1 and ABCG2 in cancer cells, and these methods are currently under investigation in our lab.

In conclusion, our findings reveal that BPD or its lipidated derivative can partially inhibit the ATPase activity of both ABCB1 and ABCG2 in a dose-dependent manner. Light activation of photosensitizers not only further reduces the ATPase activity but also induces the aggregation of the transporters due to covalent cross-linking. This study provides a first step toward understanding how photochemistry directly modulates the function of ABC drug transporters. Our results suggest that PDT technology could have a transformative impact on the field of cancer multidrug resistance. Further in vivo investigation of the photochemical inactivation of ABCB1 and ABCG2 is needed.

## ■ METHODS

**Chemicals and Reagents.** BPD was purchased from U.S. Pharmacopeia (Rockville, MD). 1-Palmitoyl-2-hydroxy-*sn*-glycero-3-phosphocholine (16:0) LysoPC was obtained from Avanti Polar Lipids (Alabaster, AL). (16:0) LysoPC-BPD was synthesized as previously described by us.[18] Monoclonal antibodies C219 and BXP-21 were purchased from Fujirebio Diagnostics, Inc. (Malvern, PA) and Enzo Life Sciences (Farmingdale, NY), respectively. All other chemicals and reagents were purchased from Thermo Fisher Scientific (Waltham, MA) or Sigma (St. Louis, MO).

**Preparation of Membrane Vesicles Containing ABC Transporters.** High Five insect cells were infected with recombinant baculovirus containing human ABCB1 or ABCG2 genes. A polyhistidine tag was added to ABCB1 (His6) and ABCG2 (His10) constructs at the C- and N-terminus, respectively. Membrane vesicles were prepared by hypotonic lysis of ABCB1- and ABCG2-expressing High Five insect cells followed by differential centrifugation, as previously described.[40] The final membrane vesicles were stored at −80 °C. Total protein concentration in membrane vesicles was measured by the Schaffner and Weissman method using amido black B dye.[41]

**Preparation of Lipid Bilayer Nanodiscs Reconstituted with ABCB1.** Human ABCB1 was reconstituted into nanodiscs as previously described.[24] Briefly, purified ABCB1, MSP1D1 protein, and *Escherichia coli* polar lipid mixture (5 mM *E. coli* lipid, 30 mM sodium cholate, 3.3 mM *n*-dodecyl-*β*-D-maltoside, 1.25 mM cholesteryl hemisuccinate) were combined at a 1:4:200 molar ratio. The mixture was incubated with bio-beads (Bio-Rad Laboratories) at 4 °C for at least 3 h with constant stirring. The nanodisc mixture was purified using a Superdex 200 increase 10/300 GL column pre-equilibrated with nanodisc buffer (25 mM *N*-(2-hydroxyethyl)piperazine-*N*′-ethanesulfonic acid pH 7.5, 150 mM NaCl, 5 mM DTT). Fractions containing one ABCB1 molecule per nanodisc were collected, concentrated by centrifugation, and stored at 4 °C.

**Photochemical Inactivation of ATPase Activity.** Membrane vesicles prepared from High Five insect cells expressing ABCB1 or ABCG2 (10 μg protein/100 μL) and lipidic nanodiscs containing purified ABCB1 (0.5 μg protein/100 μL) were resuspended in 50 mM MES-Tris buffer pH 6.8 containing 50 mM KCl, 5 mM NaN₃, 1 mM EGTA, 1 mM ouabain, 10 mM MgCl₂, and 2 mM DTT. Each sample was incubated with 0−20 μM BPD or (16:0) LysoPC-BPD, at 37 °C for 3 min and then exposed to 690 nm red light (0.05 J/cm², 50 mW/cm², Modulight). ATP hydrolysis was initiated by adding 5 mM ATP and terminated by the addition of 2.5% sodium dodecyl sulfate (SDS) after 20 min of incubation at 37 °C. Inorganic phosphate (P$_i$) reagent (1% ammonium molybdate in 2.5 N H₂SO₄ and 0.014% antimony potassium tartrate) and 0.33% sodium L-ascorbate were added to quantify the hydrolyzed Pi by measuring the absorbance at 880 nm (Amersham Biosciences). The vanadate-sensitive ATPase activity was calculated as the difference of ATPase activity in the absence or presence of 0.3 mM sodium *ortho*-vanadate. IC$_{50}$ represents the photosensitizer concentration producing half-maximal inhibition of ATPase activity.

**Gel Electrophoresis and Western Blotting.** Membrane vesicles containing ABCB1 or ABCG2 (35 μg protein/50 μL) or lipidic nanodiscs containing purified ABCB1 (1 μg protein/20 μL) were resuspended in 50 mM MES-Tris pH 6.8 containing 50 mM KCl, 5 mM NaN₃, 1 mM EGTA, 1 mM ouabain, 10 mM MgCl₂, and 2 mM DTT. Each sample was incubated with 0−20 μM BPD, or (16:0) LysoPC-BPD, at 37 °C for 3 min and then exposed to 690 nm red light (0−5 J/cm², 50 mW/cm², Modulight). To clarify the molecular mechanism underlying protein aggregation, DTT (100 mM) and urea (5 M) were added to the samples before and after light irradiation, respectively. Heat (100 °C for 3 min)-induced protein aggregation was used as a control. Protein samples were denatured by the addition of loading dye [5× loading dye contains 500 mM Tris-HCl pH 6.8, 10% SDS, 30% sucrose, 0.005% bromophenol blue and 25% (v/v) *β*-mercaptoethanol] and incubation for 20 min at 37 °C. Denaturing gel electrophoresis was conducted using a precast 7% Tris-acetate gel (for membrane vesicle samples, 10 μg protein/lane) or a precast 4−12% bis−Tris gel (for nanodisc samples, 1 μg protein/lane) at constant voltage according to the manufacturer's recommendations. Gels were stained with colloidal blue and band intensities were quantified using ImageJ and analyzed using GraphPad Prism. For western blotting, the proteins were transferred to a 0.2 μm nitrocellulose membrane for immunoblot analysis using the ABCB1-specific monoclonal antibody C219 (Fujirebio Diagnostics, Inc., Malvern, PA) or ABCG2-specific monoclonal antibody BXP-21 (1:2000; Enzo Life Sciences), as described previously.

**Reactive Oxygen Species Detection.** Reactive oxygen species generation was detected using singlet oxygen sensor green (SOSG) and hydroxyl radical and peroxynitrite sensor (HPF) for singlet oxygen and hydroxyl radical species, respectively, according to the manufacturer's instructions. Various BPD concentrations (0−20 μM) were incubated with SOSG or HPF fixed at 75 μM in a 96-well plate. Light at 690 nm (50 mW/cm², 0−5 J/cm²) was delivered vertically to the plate. A microplate reader was used to acquire the fluorescence signals of SOSG (Ex/Em: 504/525 nm) and HPF (Ex/Em: 490/515 nm) before and after light irradiation.

***In Silico* Molecular Docking Analysis.** The inward-facing structure of human ABCB1 (PDB ID: 6QEX)[42] and the structure of human ABCG2 (PDB ID: 6HCO)[5] were used for docking of BPD and (16:0) LysoPC-BPD with AutoDock Vina.[43] The following residues in the substrate-binding pocket of ABCB1 were set as flexible: L65, M68, M69, F72, Q195, W232, F303, I306, Y307, Y310, F314, F336, L339, I340, F343, Q347, N721, Q725, F728, F732, F759, F770, F938, F942, Q946, M949, Y953, F957, L975, F978, V982, F983, M986, Q990, F993, F994. The receptor grid was centered at $x = 19$, $y = 53$, and $z = 3$. For ABCG2, the following residues were set as flexible: N393, A397, N398, V401, L405, I409, T413, N424, F431, F432, T435, N436, F439, S440, V442, S443, Y538, L539, T542, I543, V546, F547, M549, I550, L554, L555. The receptor grid was centered at $x = 125$, $y = 125$, and $z = 130$. Boxes with dimensions 40 Å × 40 Å × 44 Å and 34 Å × 30 Å × 50 Å were assigned to ABCB1 and ABCG2, respectively, to search for all possible binding poses within the transmembrane region. The exhaustiveness level was set at 100 for both ABC drug transporters to ensure that the global minimum of the scoring function would be found. Analysis of the docked poses was performed using the PyMol molecular graphics system, Version 1.7 (Shrödinger, NY).

**Statistical Analysis.** All experiments were carried out at least in triplicate. Specific tests and number of repeats are indicated in the figure captions. Results are shown with mean ± SD. Statistical analyses were performed using GraphPad

Prism (GraphPad Software). Reported *P* values are two-tailed. One-way ANOVA statistical tests and appropriate posthoc analyses were applied to avoid type I errors. No exclusion criteria were used, and no data points were excluded from the analyses.

## ASSOCIATED CONTENT

**Ⓢ Supporting Information**

The Supporting Information is available free of charge at https://pubs.acs.org/doi/10.1021/acsptsci.1c00138.

> Additional data on generation of reactive oxygen species, sample temperature during light irradiation, western blotting, photochemical effects on the cysless ABCB1 mutant, gel electrophoresis of protein cross-linking in ABCG2, molecular docking analysis of BPD and (16:0) LysoPC-BPD in the substrate-binding pockets of ABCB1 and ABCG2, photochemical effects of (16:0) LysoPC-BPD on ABCB1 and ABCG2, and $IC_{50}$ values of ATPase activity inhibition (PDF)

## AUTHOR INFORMATION

**Corresponding Authors**

**Suresh V. Ambudkar** — *Laboratory of Cell Biology, Center for Cancer Research, National Cancer Institute, National Institutes of Health, Bethesda, Maryland 20892, United States*; Phone: 240-760-7192; Email: ambudkar@mail.nih.gov

**Huang-Chiao Huang** — *Fischell Department of Bioengineering, University of Maryland, College Park, Maryland 20742, United States; Marlene and Stewart Greenebaum Cancer Center, University of Maryland School of Medicine, Baltimore, Maryland 21201, United States;* Ⓞ orcid.org/0000-0002-5406-0733; Phone: 301-405-6961; Email: hchuang@umd.edu

**Authors**

**Barry J. Liang** — *Fischell Department of Bioengineering, University of Maryland, College Park, Maryland 20742, United States; Laboratory of Cell Biology, Center for Cancer Research, National Cancer Institute, National Institutes of Health, Bethesda, Maryland 20892, United States*

**Sabrina Lusvarghi** — *Laboratory of Cell Biology, Center for Cancer Research, National Cancer Institute, National Institutes of Health, Bethesda, Maryland 20892, United States*

Complete contact information is available at:
https://pubs.acs.org/10.1021/acsptsci.1c00138

**Author Contributions**

The manuscript was written through contributions of all the authors. B.J.L., S.V.A., and H.-C.H. conceived and designed experiments; B.J.L. performed experiments and analyzed data; S.L. performed *in silico* studies using AutoDock Vina; B.J.L., S.V.A., and H.-C.H. prepared the manuscript. All the authors contributed to editing the final manuscripts. All the authors have given approval to the final version of the manuscript.

**Notes**

The authors declare no competing financial interest.

## ABBREVIATIONS

ABC, ATP-binding cassette; BPD, benzoporphyrin derivative; DTT, dithiothreitol; PDT, photodynamic therapy; NBD, nucleotide-binding domain; TMD, transmembrane domain

## REFERENCES

(1) Gottesman, M. M.; Fojo, T.; Bates, S. E. Multidrug resistance in cancer: role of ATP-dependent transporters. *Nat. Rev. Canc.* **2002**, *2*, 48−58.

(2) Ambudkar, S. V.; Dey, S.; Hrycyna, C. A.; Ramachandra, M.; Pastan, I.; Gottesman, M. M. Biochemical, cellular, and pharmacological aspects of the multidrug transporter. *Annu. Rev. Pharmacol. Toxicol.* **1999**, *39*, 361−398.

(3) Robey, R. W.; Pluchino, K. M.; Hall, M. D.; Fojo, A. T.; Bates, S. E.; Gottesman, M. M. Revisiting the role of ABC transporters in multidrug-resistant cancer. *Nat. Rev. Canc.* **2018**, *18*, 452−464.

(4) Kim, Y.; Chen, J. Molecular structure of human P-glycoprotein in the ATP-bound, outward-facing conformation. *Science* **2018**, *359*, 915−919.

(5) Manolaridis, I.; Jackson, S. M.; Taylor, N. M. I.; Kowal, J.; Stahlberg, H.; Locher, K. P. Cryo-EM structures of a human ABCG2 mutant trapped in ATP-bound and substrate-bound states. *Nature* **2018**, *563*, 426−430.

(6) Kathawala, R. J.; Gupta, P.; Ashby, C. R., Jr.; Chen, Z.-S. The modulation of ABC transporter-mediated multidrug resistance in cancer: a review of the past decade. *Drug. Resist. Updat.* **2015**, *18*, 1−17.

(7) Celli, J. P.; Spring, B. Q.; Rizvi, I.; Evans, C. L.; Samkoe, K. S.; Verma, S.; Pogue, B. W.; Hasan, T. Imaging and photodynamic therapy: mechanisms, monitoring, and optimization. *Chem. Rev.* **2010**, *110*, 2795−2838.

(8) Dougherty, T. J.; Gomer, C. J.; Henderson, B. W.; Jori, G.; Kessel, D.; Korbelik, M.; Moan, J.; Peng, Q. Photodynamic therapy. *J. Natl. Canc. Inst.* **1998**, *90*, 889−905.

(9) Dolmans, D. E. J. G. J.; Fukumura, D.; Jain, R. K. Photodynamic therapy for cancer. *Nat. Rev. Canc.* **2003**, *3*, 380−387.

(10) Agostinis, P.; Berg, K.; Cengel, K. A.; Foster, T. H.; Girotti, A. W.; Gollnick, S. O.; Hahn, S. M.; Hamblin, M. R.; Juzeniene, A.; Kessel, D.; Korbelik, M.; Moan, J.; Mroz, P.; Nowis, D.; Piette, J.; Wilson, B. C.; Golab, J. Photodynamic therapy of cancer: an update. *CA Canc. J. Clin.* **2011**, *61*, 250−281.

(11) Shimada, K.; Matsuda, S.; Jinno, H.; Kameyama, N.; Konno, T.; Arai, T.; Ishihara, K.; Kitagawa, Y. The Noninvasive Treatment for Sentinel Lymph Node Metastasis by Photodynamic Therapy Using Phospholipid Polymer as a Nanotransporter of Verteporfin. *Biomed. Res. Int.* **2017**, *8*, 7412865.

(12) Spring, B. Q.; Abu-Yousif, A. O.; Palanisami, A.; Rizvi, I.; Zheng, X.; Mai, Z.; Anbil, S.; Sears, R. B.; Mensah, L. B.; Goldschmidt, R.; Erdem, S. S.; Oliva, E.; Hasan, T. Selective treatment and monitoring of disseminated cancer micrometastases in vivo using dual-function, activatable immunoconjugates. *Proc. Natl. Acad. Sci. U.S.A.* **2014**, *111*, E933−E942.

(13) Cengel, K. A.; Glatstein, E.; Hahn, S. M. Intraperitoneal photodynamic therapy. *Canc. Treat. Res.* **2007**, *134*, 493−514.

(14) Jonker, J. W.; Buitelaar, M.; Wagenaar, E.; Van Der Valk, M. A.; Scheffer, G. L.; Scheper, R. J.; Plosch, T.; Kuipers, F.; Elferink, R. P. J. O.; Rosing, H.; Beijnen, J. H.; Schinkel, A. H. The breast cancer

resistance protein protects against a major chlorophyll-derived dietary phototoxin and protoporphyria. *Proc. Natl. Acad. Sci. U.S.A.* **2002**, *99*, 15649−15654.

(15) Robey, R. W.; Steadman, K.; Polgar, O.; Bates, S. E. ABCG2-mediated transport of photosensitizers: potential impact on photodynamic therapy. *Canc. Biol. Ther.* **2005**, *4*, 187−194.

(16) Gallagher-Colombo, S. M.; Miller, J.; Cengel, K. A.; Putt, M. E.; Vinogradov, S. A.; Busch, T. M. Erlotinib Pretreatment Improves Photodynamic Therapy of Non-Small Cell Lung Carcinoma Xenografts via Multiple Mechanisms. *Canc. Res.* **2015**, *75*, 3118−3126.

(17) Palasuberniam, P.; Yang, X.; Kraus, D.; Jones, P.; Myers, K. A.; Chen, B. ABCG2 transporter inhibitor restores the sensitivity of triple negative breast cancer cells to aminolevulinic acid-mediated photodynamic therapy. *Sci. Rep.* **2015**, *5*, 13298.

(18) Baglo, Y.; Liang, B. J.; Robey, R. W.; Ambudkar, S. V.; Gottesman, M. M.; Huang, H.-C. Porphyrin-lipid assemblies and nanovesicles overcome ABC transporter-mediated photodynamic therapy resistance in cancer cells. *Canc. Lett.* **2019**, *457*, 110−118.

(19) Dickinson, B. C.; Chang, C. J. Chemistry and biology of reactive oxygen species in signaling or stress responses. *Nat. Chem. Biol.* **2011**, *7*, 504−511.

(20) Huang, H.-C.; Mallidi, S.; Liu, J.; Chiang, C.-T.; Mai, Z.; Goldschmidt, R.; Ebrahim-Zadeh, N.; Rizvi, I.; Hasan, T. Photodynamic Therapy Synergizes with Irinotecan to Overcome Compensatory Mechanisms and Improve Treatment Outcomes in Pancreatic Cancer. *Cancer Res.* **2016**, *76*, 1066−1077.

(21) Mao, C.; Li, F.; Zhao, Y.; Debinski, W.; Ming, X. P-glycoprotein-targeted photodynamic therapy boosts cancer nanomedicine by priming tumor microenvironment. *Theranostics* **2018**, *8*, 6274−6290.

(22) Ambudkar, S. V.; Kimchi-Sarfaty, C.; Sauna, Z. E.; Gottesman, M. M. P-glycoprotein: from genomics to mechanism. *Oncogene* **2003**, *22*, 7468−7485.

(23) Sim, H.-M.; Bhatnagar, J.; Chufan, E. E.; Kapoor, K.; Ambudkar, S. V. Conserved Walker A cysteines 431 and 1074 in human P-glycoprotein are accessible to thiol-specific agents in the apo and ADP-vanadate trapped conformations. *Biochemistry* **2013**, *52*, 7327−7338.

(24) Nandigama, K.; Lusvarghi, S.; Shukla, S.; Ambudkar, S. V. Large-scale purification of functional human P-glycoprotein (ABCB1). *Protein Expr. Purif.* **2019**, *159*, 60−68.

(25) Goler-Baron, V.; Assaraf, Y. G. Overcoming multidrug resistance via photodestruction of ABCG2-rich extracellular vesicles sequestering photosensitive chemotherapeutics. *PLoS One* **2012**, *7*, No. e35487.

(26) Spring, B. Q.; Rizvi, I.; Xu, N.; Hasan, T. The role of photodynamic therapy in overcoming cancer drug resistance. *Photochem. Photobiol. Sci.* **2015**, *14*, 1476−1491.

(27) Aniogo, E. C.; Plackal Adimuriyil George, B.; Abrahamse, H. The role of photodynamic therapy on multidrug resistant breast cancer. *Canc. Cell Int.* **2019**, *19*, 91.

(28) Nosol, K.; Romane, K.; Irobalieva, R. N.; Alam, A.; Kowal, J.; Fujita, N.; Locher, K. P. Cryo-EM structures reveal distinct mechanisms of inhibition of the human multidrug transporter ABCB1. *Proc. Natl. Acad. Sci. U.S.A.* **2020**, *117*, 26245−26253.

(29) Morgan, J.; Jackson, J. D.; Zheng, X.; Pandey, S. K.; Pandey, R. K. Substrate affinity of photosensitizers derived from chlorophyll-a: the ABCG2 transporter affects the phototoxic response of side population stem cell-like cancer cells to photodynamic therapy. *Mol. Pharm.* **2010**, *7*, 1789−1804.

(30) Davies, M. J.; Truscott, R. J. W. Photo-oxidation of proteins and its consequences. In *Comprehensive Series in Photosciences*; Giacomoni, P. U., Ed.; Elsevier, 2001; Chapter 12, pp 251−275.

(31) Verweij, H.; Dubbelman, T. M. A. R.; Van Steveninck, J. Photodynamic protein cross-linking. *Biochim. Biophys. Acta* **1981**, *647*, 87−94.

(32) Shen, H.-R.; Spikes, J. D.; Kopečeková, P.; Kopeček, J. Photodynamic crosslinking of proteins. I. Model studies using

histidine- and lysine-containing N-(2-hydroxypropyl)methacrylamide copolymers. *J. Photochem. Photobiol. B* **1996**, *34*, 203−210.

(33) Konstantinou, E. K.; Notomi, S.; Kosmidou, C.; Brodowska, K.; Al-Moujahed, A.; Nicolaou, F.; Tsoka, P.; Gragoudas, E.; Miller, J. W.; Young, L. H.; Vavvas, D. G. Verteporfin-induced formation of protein cross-linked oligomers and high molecular weight complexes is mediated by light and leads to cell toxicity. *Sci. Rep.* **2017**, *7*, 46581.

(34) Davies, M. J. Protein oxidation and peroxidation. *Biochem. J.* **2016**, *473*, 805−825.

(35) Urbatsch, I. L.; Gimi, K.; Wilke-Mounts, S.; Lerner-Marmarosh, N.; Rousseau, M.-E.; Gros, P.; Senior, A. E. Cysteines 431 and 1074 are responsible for inhibitory disulfide cross-linking between the two nucleotide-binding sites in human P-glycoprotein. *J. Biol. Chem.* **2001**, *276*, 26980−26987.

(36) Girotti, A. W. Photosensitized oxidation of membrane lipids: reaction pathways, cytotoxic effects, and cytoprotective mechanisms. *J. Photochem. Photobiol. B* **2001**, *63*, 103−113.

(37) Vignoni, M.; Urrutia, M. N.; Junqueira, H. C.; Greer, A.; Reis, A.; Baptista, M. S.; Itri, R.; Thomas, A. H. Photo-Oxidation of Unilamellar Vesicles by a Lipophilic Pterin: Deciphering Biomembrane Photodamage. *Langmuir* **2018**, *34*, 15578−15586.

(38) Liang, B. J.; Pigula, M.; Baglo, Y.; Najafali, D.; Hasan, T.; Huang, H.-C. Breaking the selectivity-uptake trade-off of photoimmunoconjugates with nanoliposomal irinotecan for synergistic multi-tier cancer targeting. *J. Nanobiotechnol.* **2020**, *18*, 1.

(39) Baglo, Y.; Sorrin, A. J.; Liang, B. J.; Huang, H. C. Harnessing the Potential Synergistic Interplay Between Photosensitizer Dark Toxicity and Chemotherapy. *Photochem. Photobiol.* **2020**, *96*, 636−645.

(40) Ambudkar, S. V. Drug-stimulatable ATPase activity in crude membranes of human MDR1-transfected mammalian cells. *Methods Enzymol.* **1998**, *292*, 504−514.

(41) Schaffner, W.; Weissmann, C. A rapid, sensitive, and specific method for the determination of protein in dilute solution. *Anal. Biochem.* **1973**, *56*, 502−514.

(42) Alam, A.; Kowal, J.; Broude, E.; Roninson, I.; Locher, K. P. Structural insight into substrate and inhibitor discrimination by human P-glycoprotein. *Science* **2019**, *363*, 753−756.

(43) Trott, O.; Olson, A. J. AutoDock Vina: improving the speed and accuracy of docking with a new scoring function, efficient optimization, and multithreading. *J. Comput. Chem.* **2010**, *31*, 455−461.